Laboratoř růstových regulátorů

Miroslav Strnad

Respirace a metabolismus lipidů [kap. 11]

- Univerzita Palackého & Ústav experimentální botaniky AV CR

FIGURE 11.1 Overview of respiration. Substrates for respiration are generated by other cellular processes and enter the respiratory pathways. Glycolysis and the pentose phosphate pathways in the cytosol and plastid convert sugars to organic acids, via hexose phosphates and triose phosphates, generating NADH or NADPH and ATP. The organic acids are oxidized in the mitochondrial citric acid cycle, and the NADH and $FADH_2$ produced provide the energy for ATP synthesis by the electron transport chain and ATP synthase in oxidative phosphorylation. In gluconeogenesis, carbon from lipid breakdown is broken down in the glyoxysomes, metabolized in the citric acid cycle, and then used to synthesize sugars in the cytosol by reverse glycolysis.

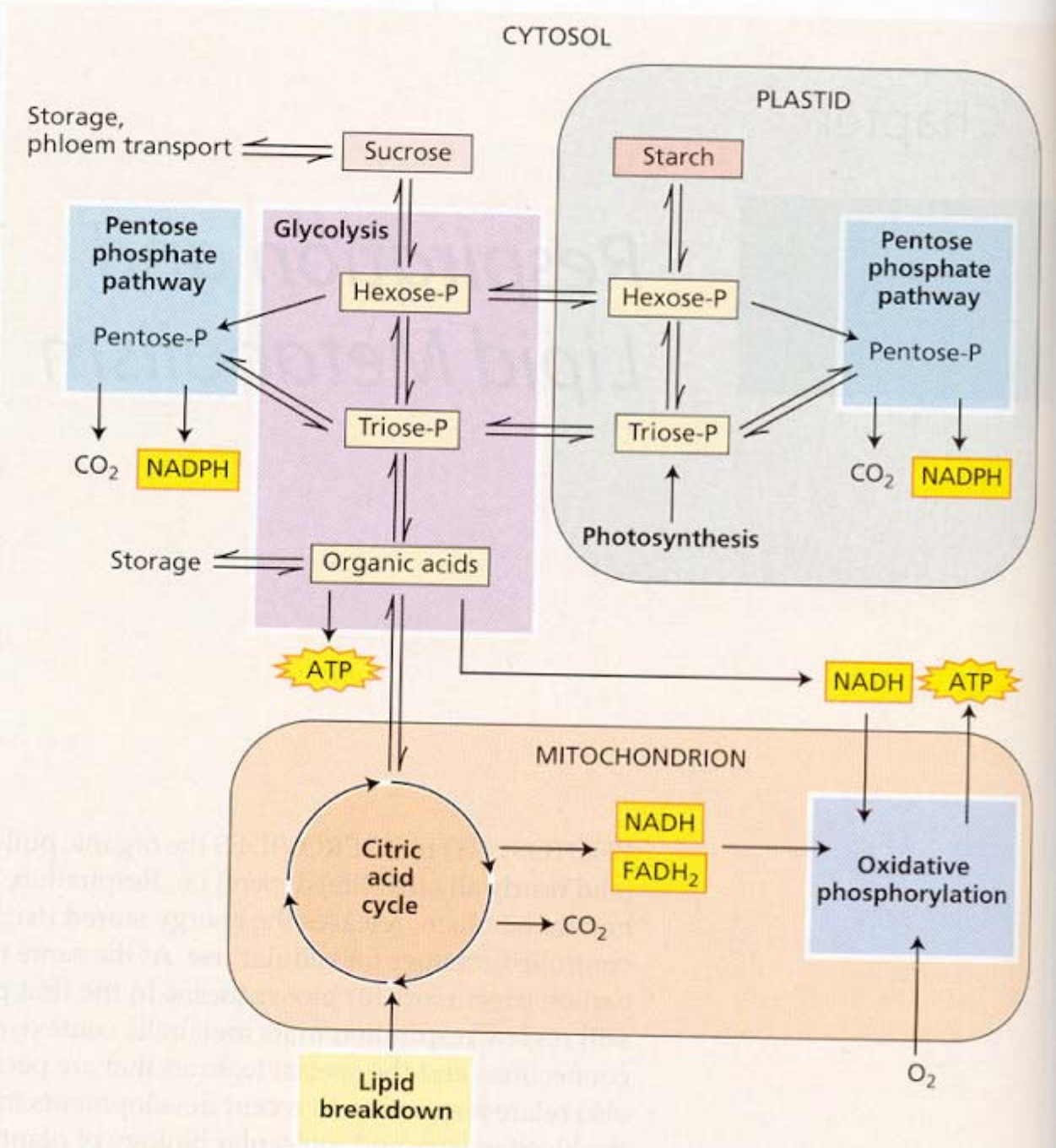

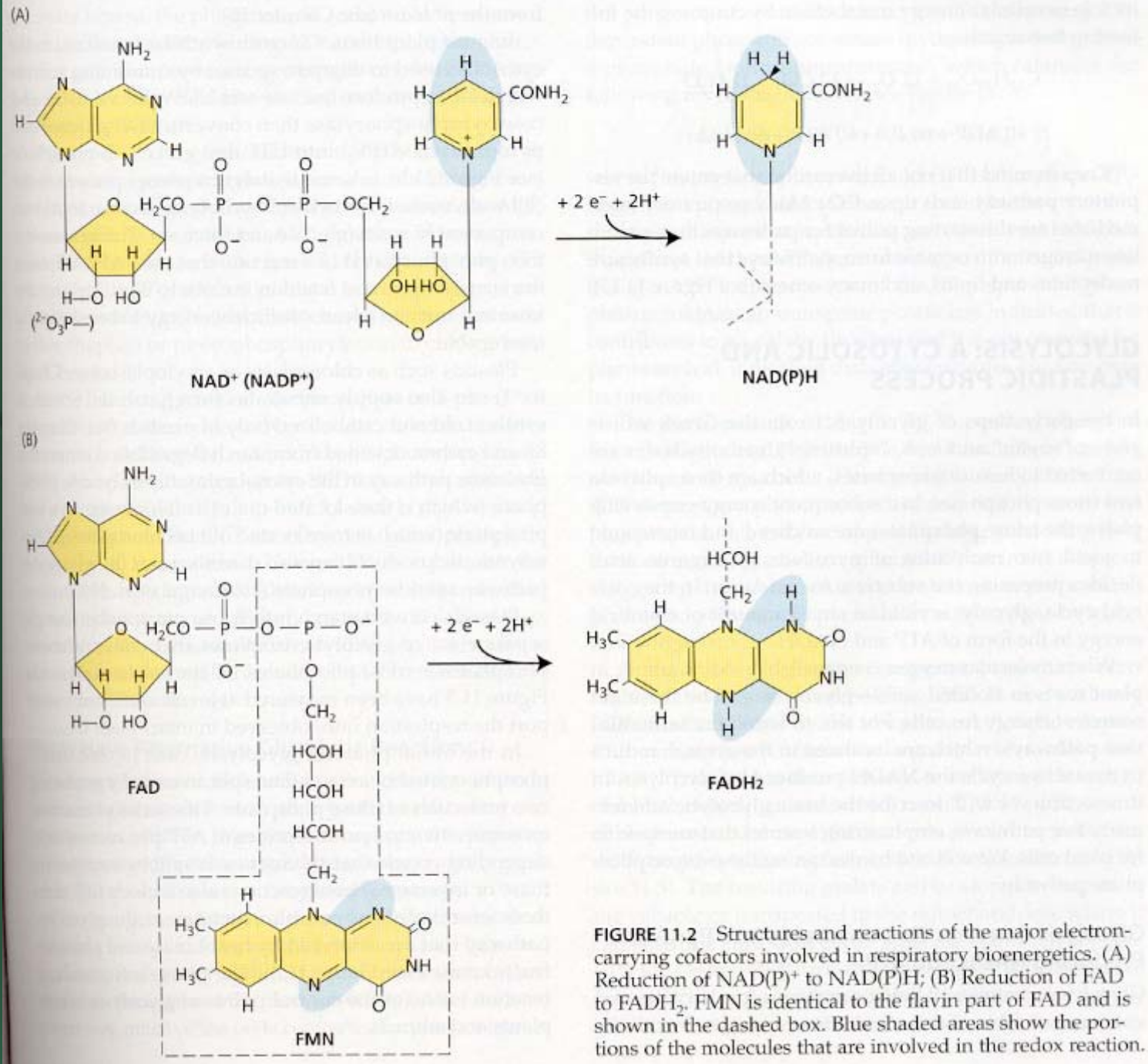

FIGURE 11.2 Structures and reactions of the major electron-carrying cofactors involved in respiratory bioenergetics. (A) Reduction of $NAD(P)^+$ to NAD(P)H; (B) Reduction of FAD to $FADH_2$. FMN is identical to the flavin part of FAD and is shown in the dashed box. Blue shaded areas show the portions of the molecules that are involved in the redox reaction.

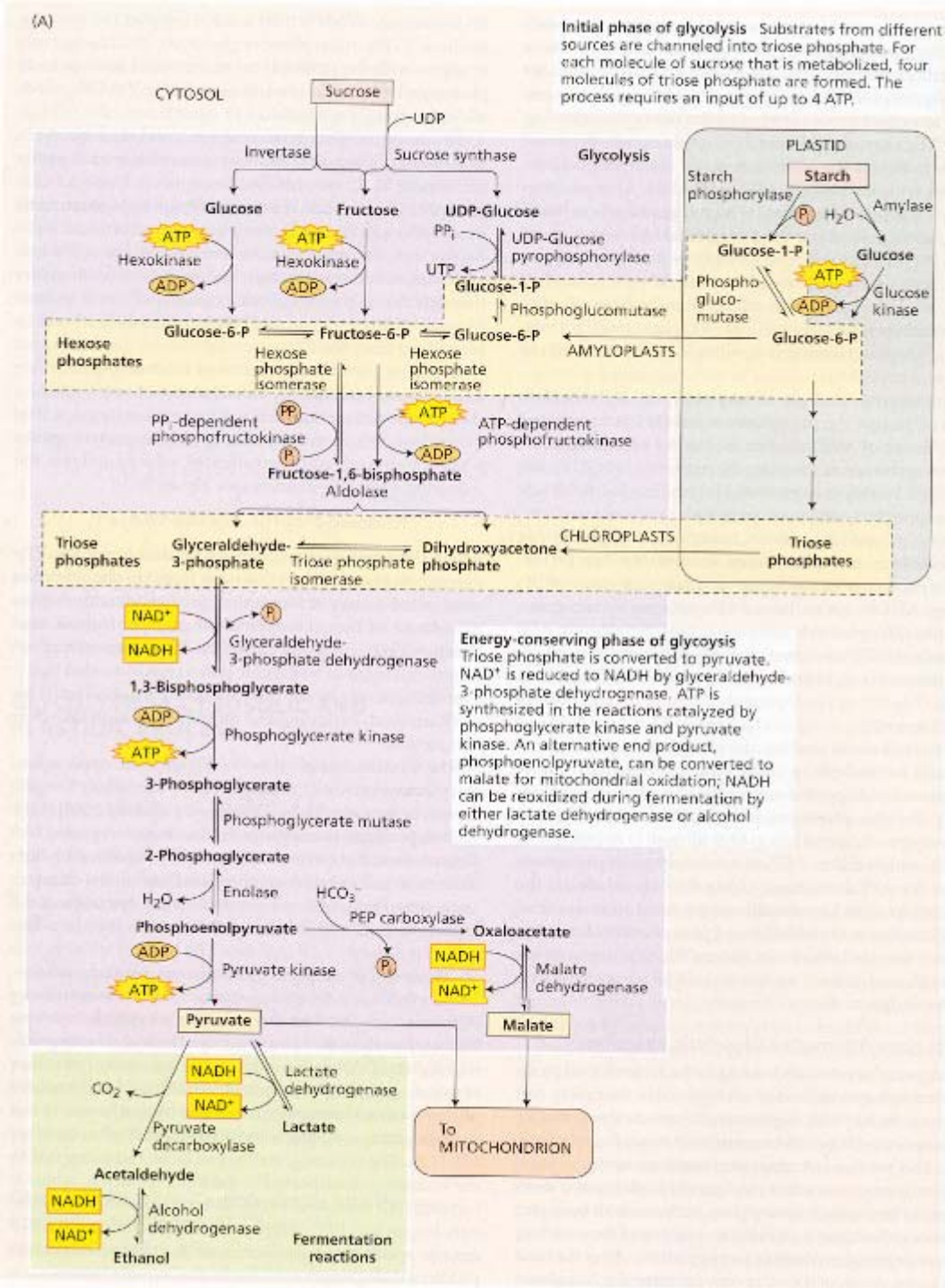

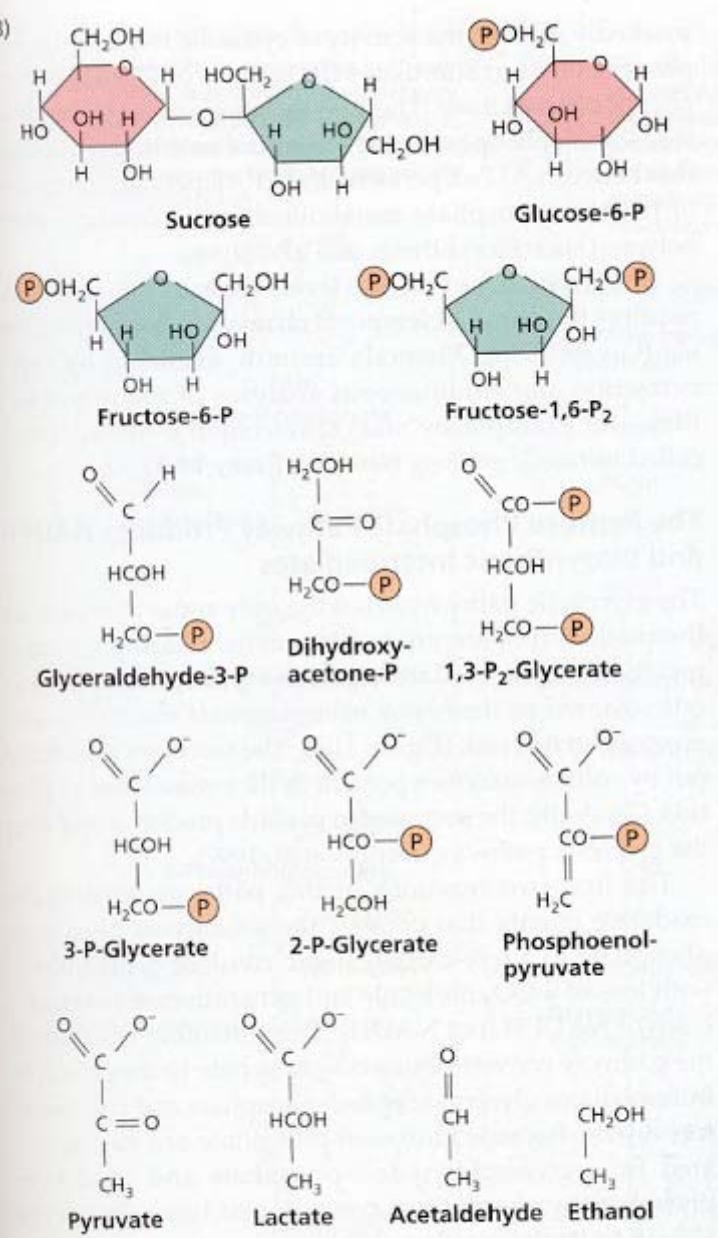

FIGURE 11.3 Reactions of plant glycolysis and fermentation. (A) In the main pathway, sucrose is oxidized to the organic acid pyruvate. The double arrows denote reversible reactions; the single arrows, essentially irreversible reactions. (B) The structures of the intermediates. P, phosphate; P_2, bisphosphate.

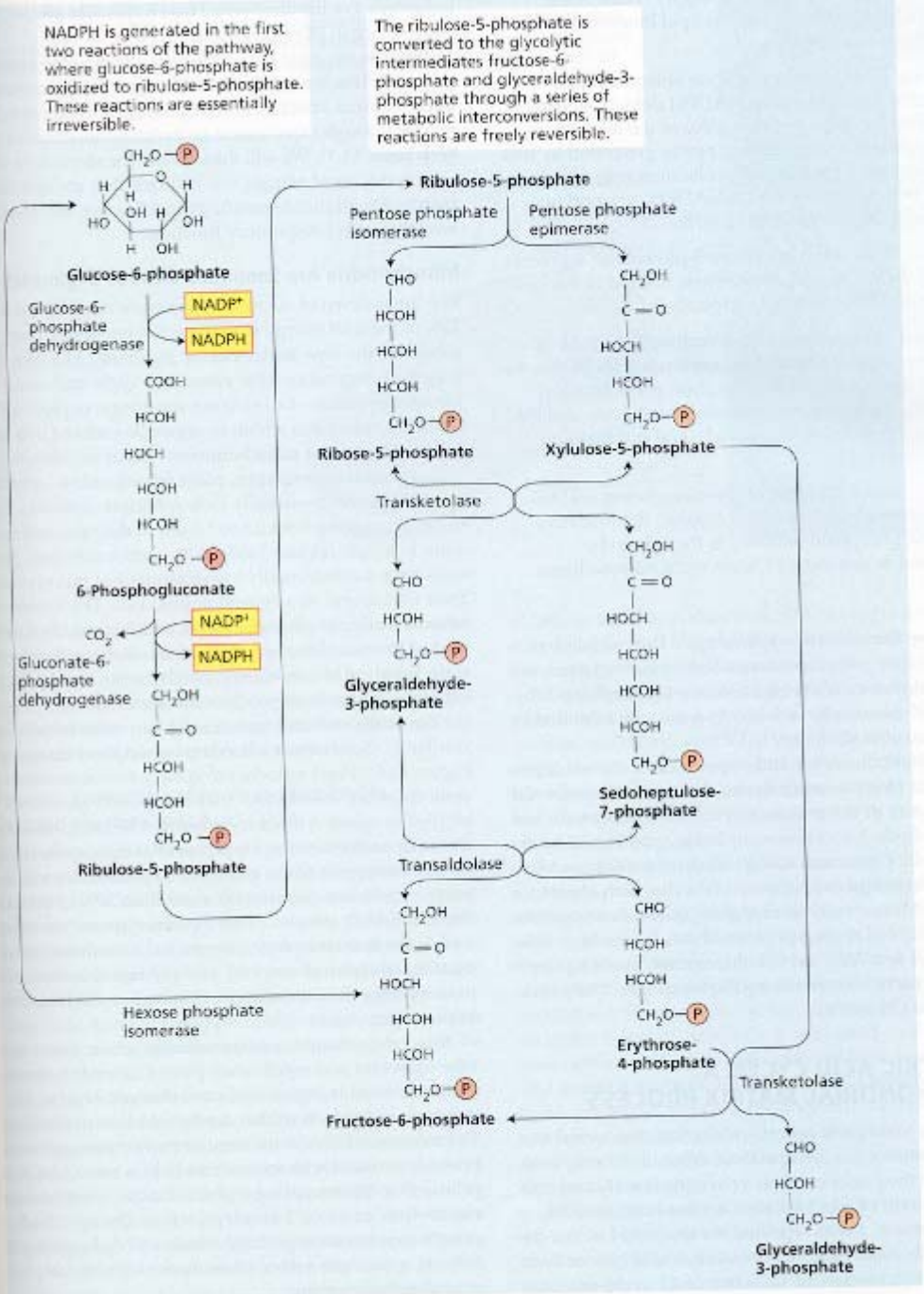

FIGURE 11.4 Reactions of the oxidative pentose phosphate pathway in higher plants. P, phosphate.

FIGURE 11.5 Structure of plant mitochondria. (A) Three-dimensional representation of a mitochondrion, showing the invaginations of the inner membrane that are called cristae, as well as the location of the matrix and intermembrane spaces (see also Figure 11.10). (B) Electron micrograph of mitochondria in a mesophyll cell of *Vicia faba*. (Photo from Gunning and Steer 1996.)

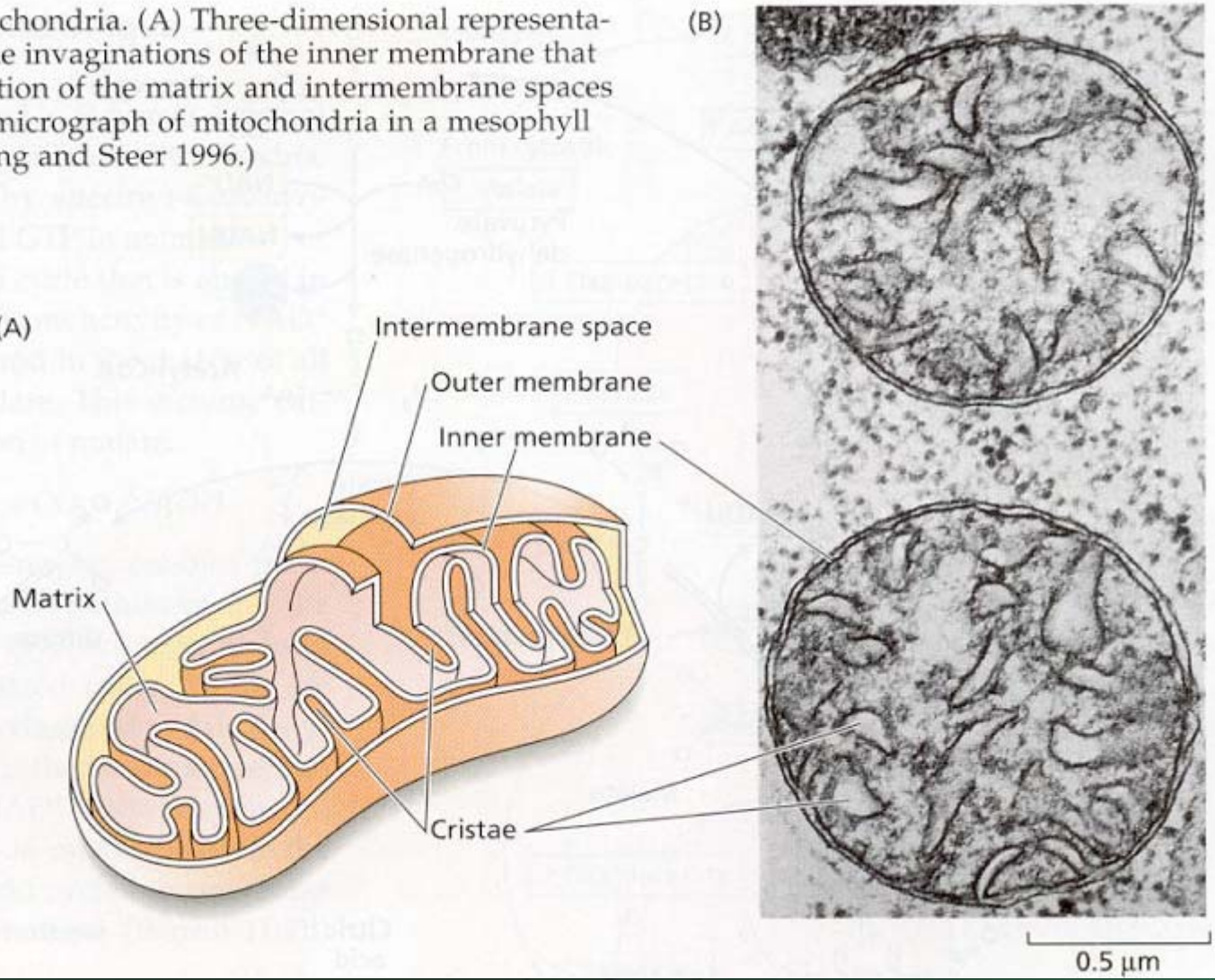

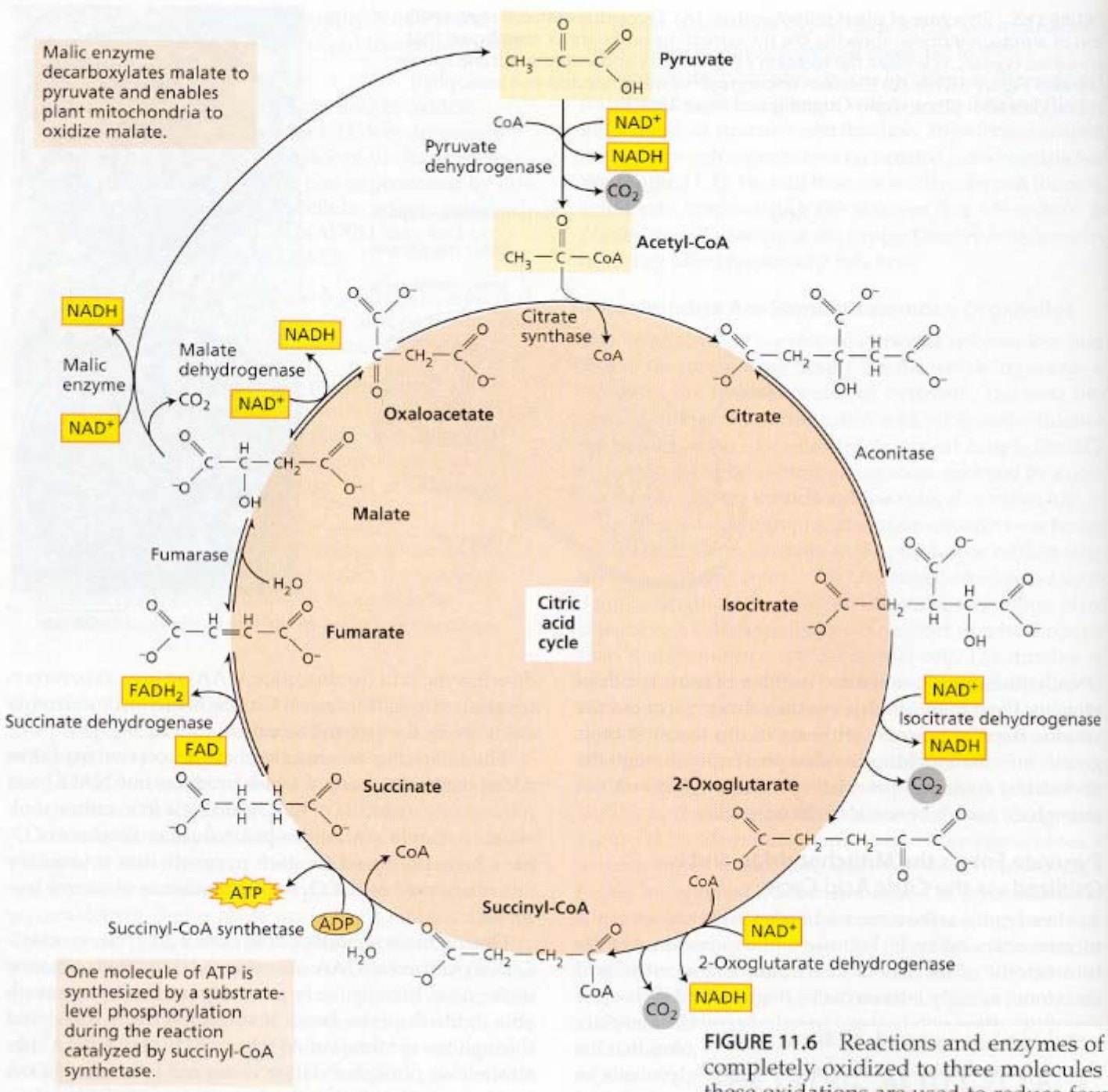

FIGURE 11.6 Reactions and enzymes of the plant citric acid cycle. Pyruvate is completely oxidized to three molecules of CO_2. The electrons released during these oxidations are used to reduce four molecules of NAD^+ to NADH and one molecule of FAD to $FADH_2$.

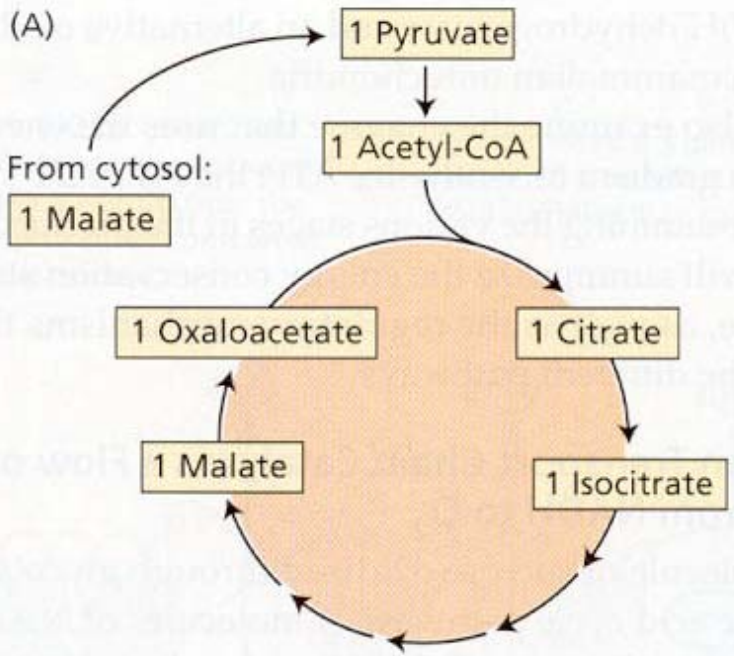

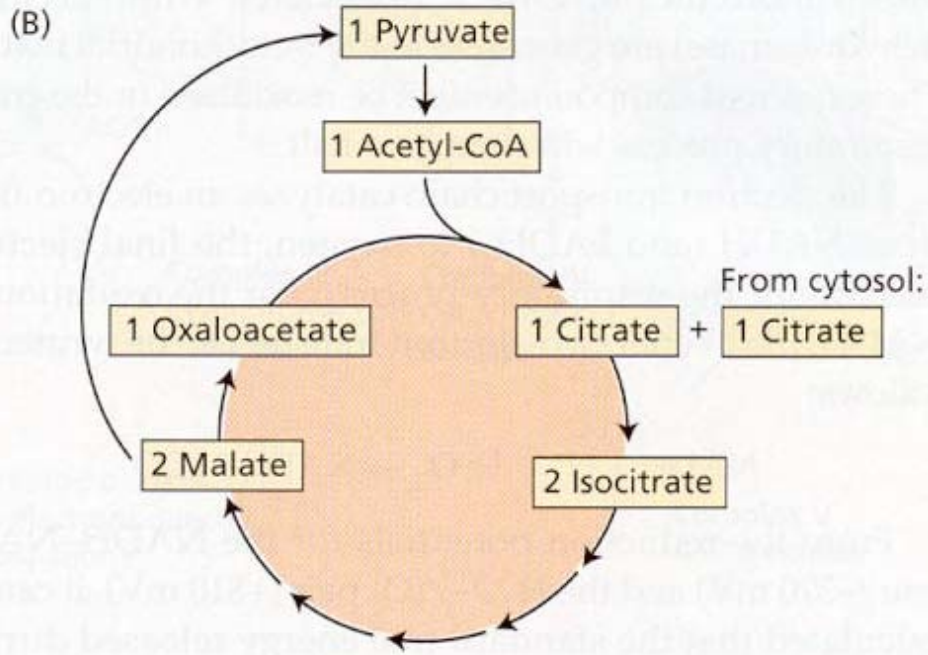

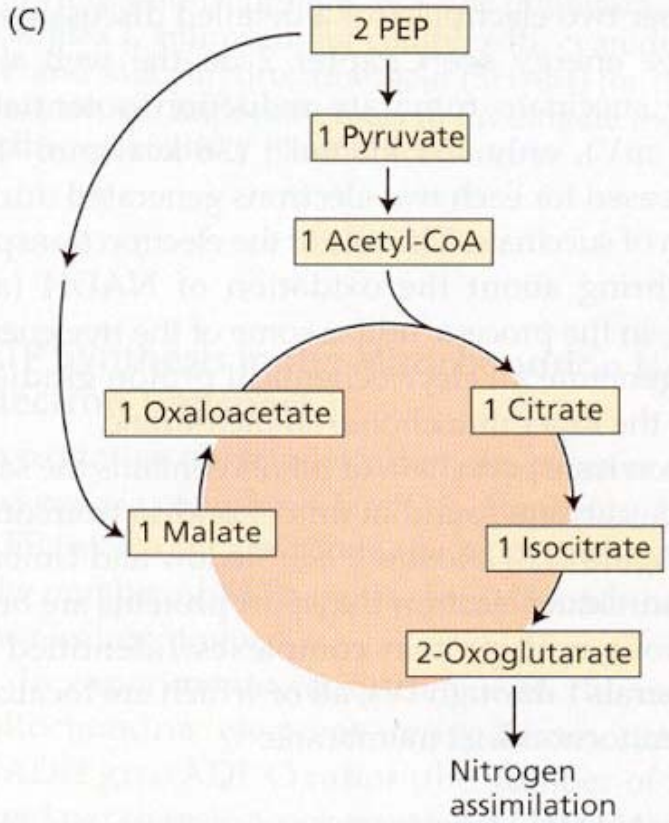

FIGURE 11.7 Malic enzyme and PEP carboxylase provide plants with metabolic flexibility for the metabolism of phosphoenolpyruvate. Malic enzyme makes it possible for plant mitochondria to oxidize both malate (A) and citrate (B) to CO_2 without involving pyruvate delivered by glycolysis. The joint action of PEP carboxylase and pyruvate kinase can convert glycolytic PEP to 2-oxoglutarate, which is used for nitrogen assimilation (C).

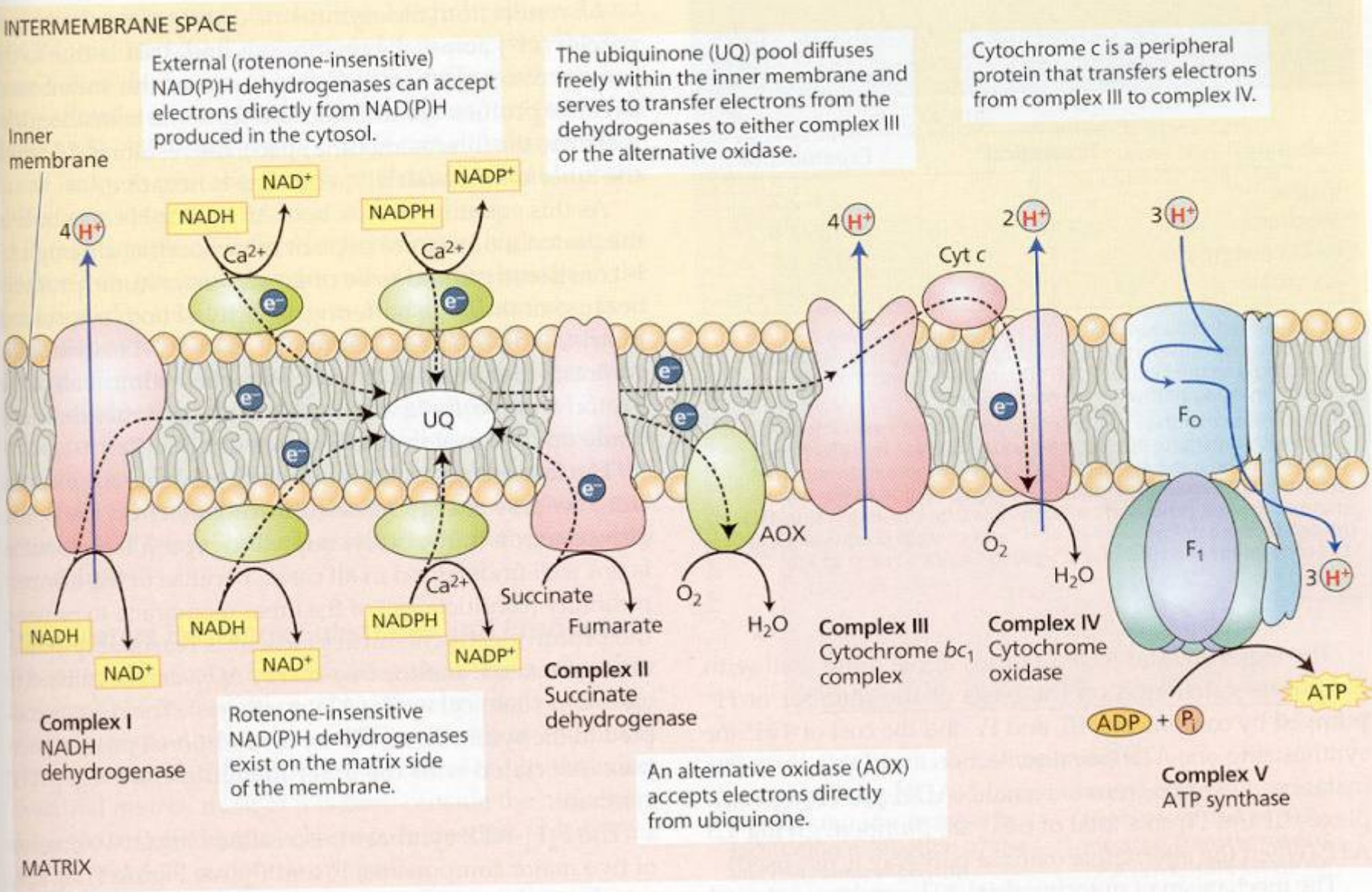

FIGURE 11.8 Organization of the electron transport chain and ATP synthesis in the inner membrane of plant mitochondria. In addition to the five standard protein complexes found in nearly all other mitochondria, the electron transport chain of plant mitochondria contains five additional enzymes marked in green. None of these additional enzymes pumps protons. Specific inhibitors, rotenone for complex I, antimycin for complex III, cyanide for complex IV, and salicylhydroxamic acid (SHAM) for the alternative oxidase, are important tools to investigate the electron transport chain of plant mitochondria.

1. Addition of succinate initiates mitochondrial electron transfer, which is measured with an oxygen electrode as the rate of oxygen reduction (to H_2O).

2. Addition of cyanide inhibits electron flow through the main cytochrome pathway and only allows electron flow to oxygen through the alternative, cyanide-resistant pathway, which is subsequently inhibited by the addition of SHAM.

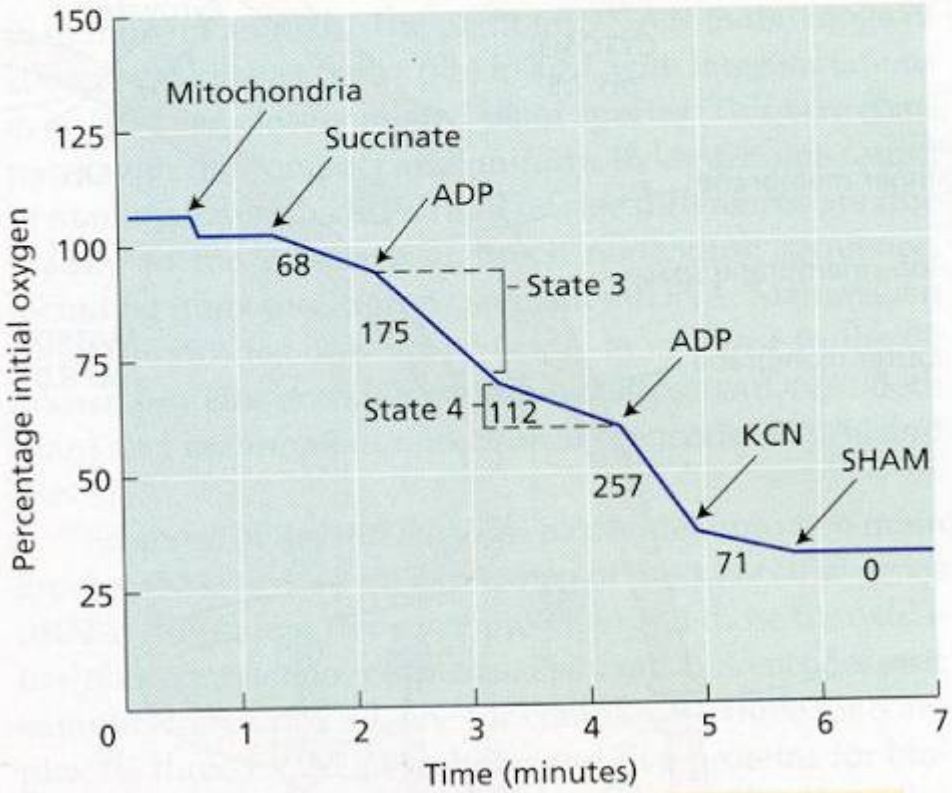

TABLE 11.1
Theoretical and experimental ADP:O ratios in isolated plant mitochondria

Substrate	ADP:O ratio	
	Theoretical[a]	Experimental
Malate	2.5	2.4–2.7
Succinate	1.5	1.6–1.8
NADH (external)	1.5	1.6–1.8
Ascorbate	1.0[b]	0.8–0.9

3. Addition of ADP stimulates electron transfer (state 3) by facilitating dissipation of the electrochemical proton gradient. The rate is higher after the second ADP addition because of activation of succinate dehydrogenase.

4. When all the ADP has been converted to ATP, electron transfer reverts to a lower rate (state 4).

FIGURE 11.9 Regulation of respiratory rate by ADP during succinate oxidation in isolated mitochondria from mung bean (*Vigna radiata*). The numbers below the traces are the rates of oxygen uptake expressed as O_2 consumed (nmol min^{-1} mg $protein^{-1}$). (Data courtesy of Steven J. Stegink.)

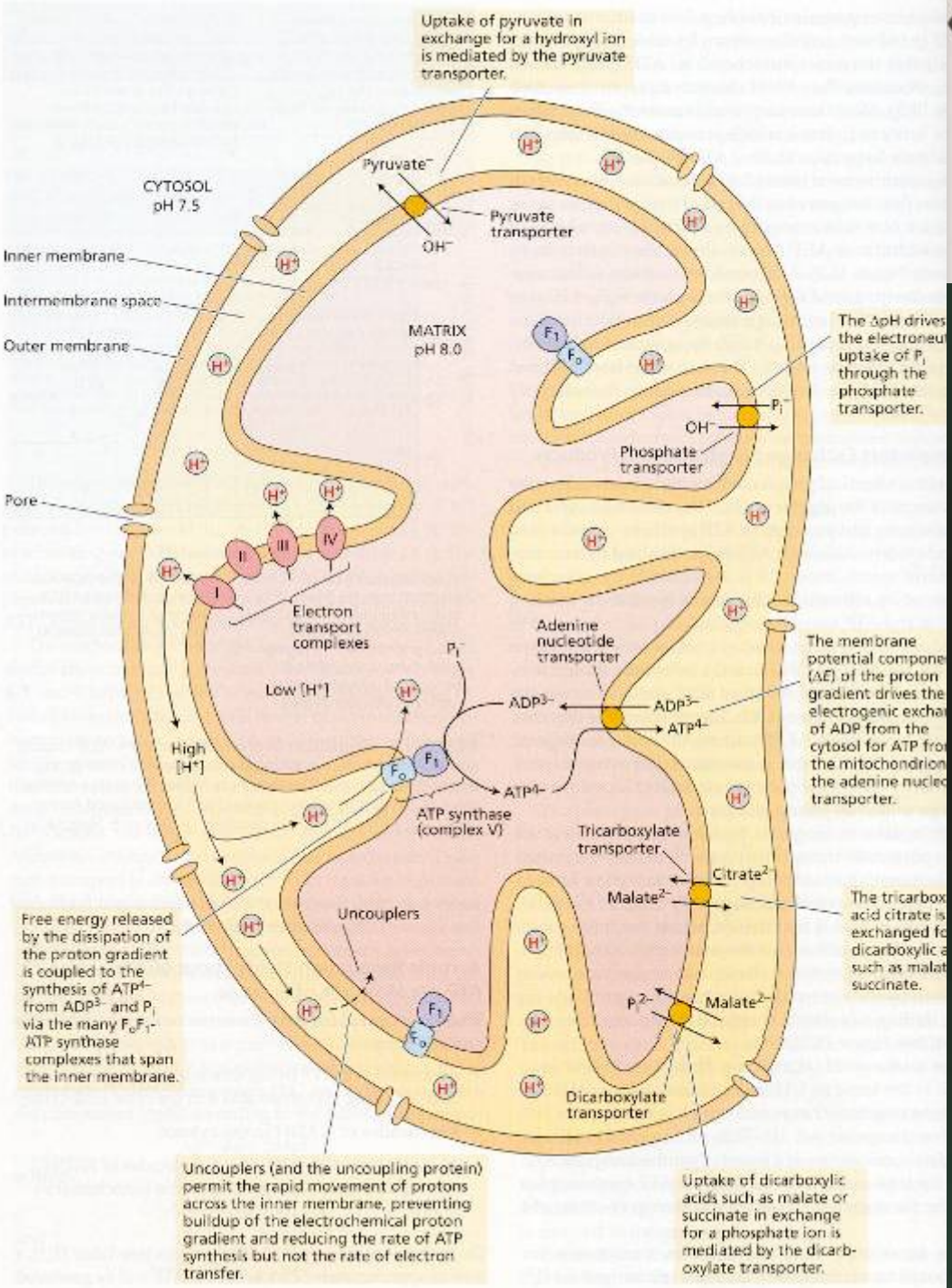

FIGURE 11.10 Transmembrane transport in plant mitochondria. An electrochemical proton gradient ($\Delta\tilde{\mu}_{H^+}$) consisting of a membrane potential (ΔE, –200mV, negative inside) and a ΔpH (alkaline inside) is established across the inner mitochondrial membrane during electron transport as outlined in the text. Specific metabolites are moved across the inner membrane by specialized proteins, called transporters or carriers (After Douce 1985).

TABLE 11.2
The maximum yield of cytosolic ATP from the complete oxidation of sucrose to CO_2 via aerobic glycolysis and the citric acid cycle

Part reaction		ATP per sucrose[a]
Glycolysis		
4 substrate-level phosphorylations		4
4 NADH	4 ×1.5	6
Citric acid cycle		
4 substrate level phosphorylations		4
4 $FADH_2$	4 × 1.5	6
16 NADH	16 × 2.5	40
Total		60

Source: Adapted from Brand 1994.

Note: Cytosolic NADH is assumed oxidized by the external NADH dehydrogenase. The nonphosphorylating pathways are assumed not to be engaged.

[a]Calculated using the theoretical values from Table 11.1

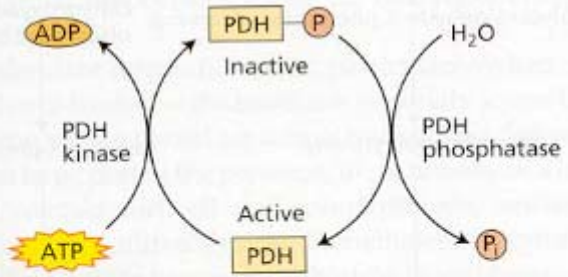

Pyruvate + CoA + NAD^+ ⟶ Acetyl-CoA + CO_2 + NADH

Effect on PDH activity	Mechanism
Activating	
Pyruvate	Inhibits kinase
ADP	Inhibits kinase
Mg^{2+} (or Mn^{2+})	Stimulates phosphatase
Inactivating	
NADH	Inhibits PDH Stimulates kinase
Acetyl CoA	Inhibits PDH Stimulates kinase
NH_4^+	Inhibits PDH Stimulates kinase

FIGURE 11.11 Regulation of pyruvate dehydrogenase (PDH) activity by reversible phosphorylation and by other metabolites.

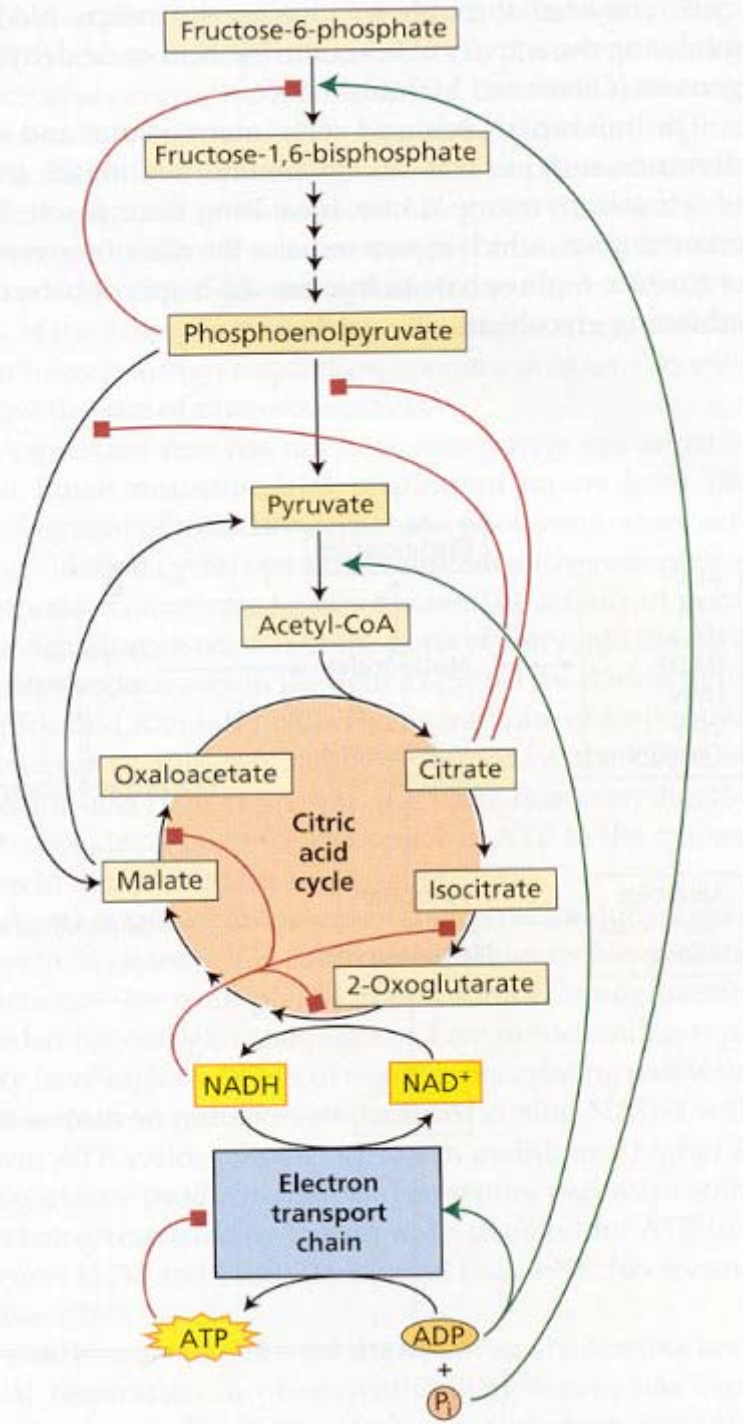

FIGURE 11.12 Concept of bottom-up regulation of plant respiration. Several substrates for respiration (e.g., ADP) stimulate enzymes in early steps of the pathways (green arrows). In contrast, accumulation of products (e.g., ATP) inhibits (red squares) earlier reactions in a stepwise fashion. For instance, ATP inhibits the electron transport chain leading to an accumulation of NADH. NADH inhibits citric acid enzymes such as isocitrate dehydrogenase and 2-oxoglutarate dehydrogenase. Then, citric acid cycle intermediates like citrate inhibit the PEP-metabolizing enzymes in the cytosol. Finally, PEP inhibits the conversion of fructose-6-phosphate to fructose-1,6-biphosphate and restricts carbon feeding into glycolysis.

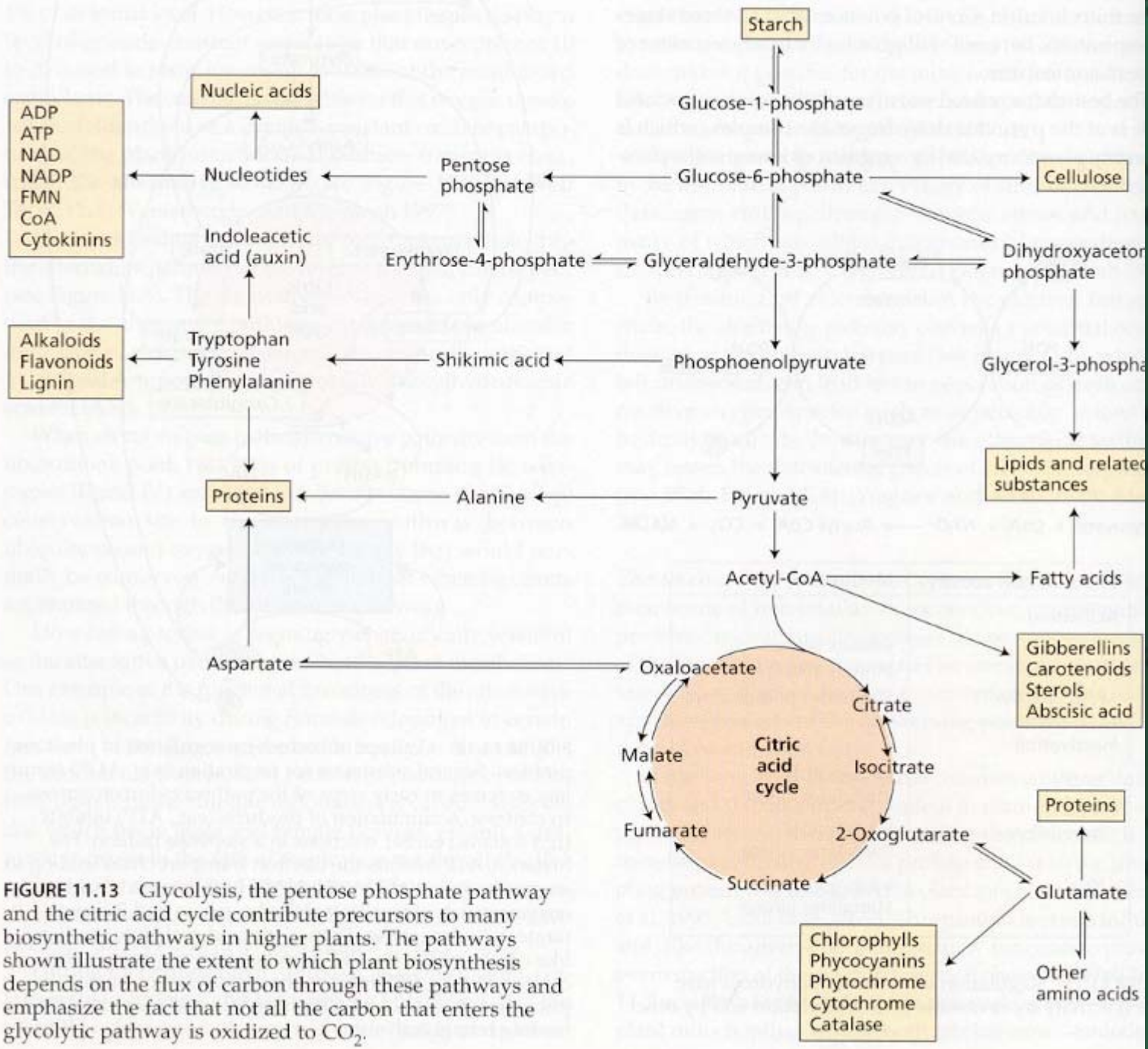

FIGURE 11.13 Glycolysis, the pentose phosphate pathway and the citric acid cycle contribute precursors to many biosynthetic pathways in higher plants. The pathways shown illustrate the extent to which plant biosynthesis depends on the flux of carbon through these pathways and emphasize the fact that not all the carbon that enters the glycolytic pathway is oxidized to CO_2.

FIGURE 11.14 Structural features of triacylglycerols and polar glycerolipids in higher plants. The carbon chain lengths of the fatty acids, which always have an even number of carbons, range from 12 to 20 but are typically 16 or 18. Thus, the value of n is usually 14 or 16.

Glycerol

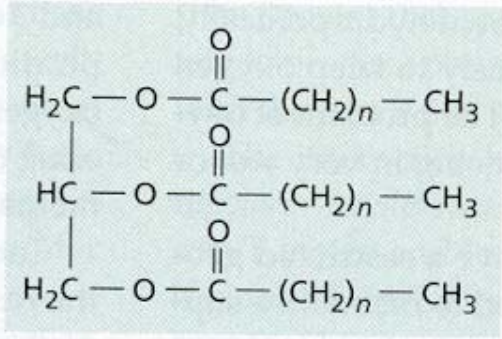

Triacylglycerol
(the major stored lipid)

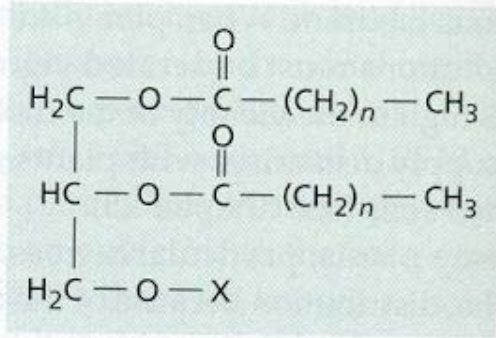

Glycerolipid

X = H	Diacylglycerol (DAG)
X = HPO_3^{2-}	Phosphatidic acid
X = $PO_3^{2-} — CH_2 — CH_2 — \overset{+}{N}(CH_3)_3$	Phosphatidylcholine
X = $PO_3^{2-} — CH_2 — CH_2 — NH_2$	Phosphatidylethanolamine
X = galactose	Galactolipids

TABLE 11.3
Common fatty acids in higher plant tissues

Name[a]	Structure
Saturated Fatty Acids	
Lauric acid (12:0)	$CH_3(CH_2)_{10}CO_2H$
Myristic acid (14:0)	$CH_3(CH_2)_{12}CO_2H$
Palmitic acid (16:0)	$CH_3(CH_2)_{14}CO_2H$
Stearic acid (18:0)	$CH_3(CH_2)_{16}CO_2H$
Unsaturated Fatty Acids	
Oleic acid (18:1)	$CH_3(CH_2)_7CH=CH(CH_2)_7CO_2H$
Linoleic acid (18:2)	$CH_3(CH_2)_4CH=CH-CH_2-CH=CH(CH_2)_7CO_2H$
Linolenic acid (18:3)	$CH_3CH_2CH=CH-CH_2-CH=CH-CH_2-CH=CH-(CH_2)_7CO_2H$

[a]Each fatty acid has a numerical abbreviation. The number before the colon represents the total number of carbons; the number after the colon is the number of double bonds.

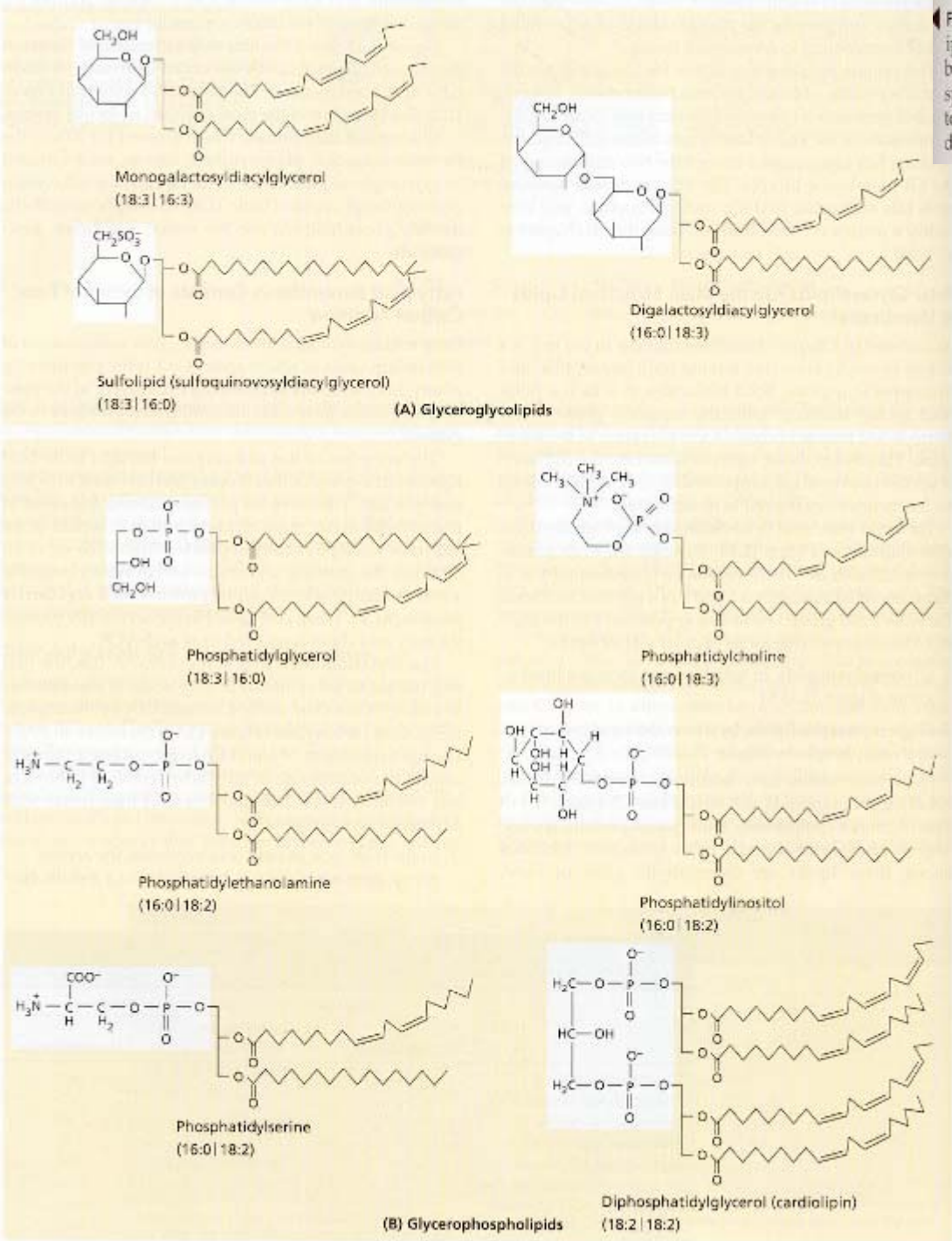

FIGURE 11.15 Major polar lipids of plant membranes: (A) glyceroglycolipids and (B) glycerophospholipids. At least six different fatty acids may be attached to the glycerol backbone. One of the more common molecular species is shown for each lipid. The numbers given below each name refer to the number of carbons (number before the colon) and the number of double bonds (number after the colon).

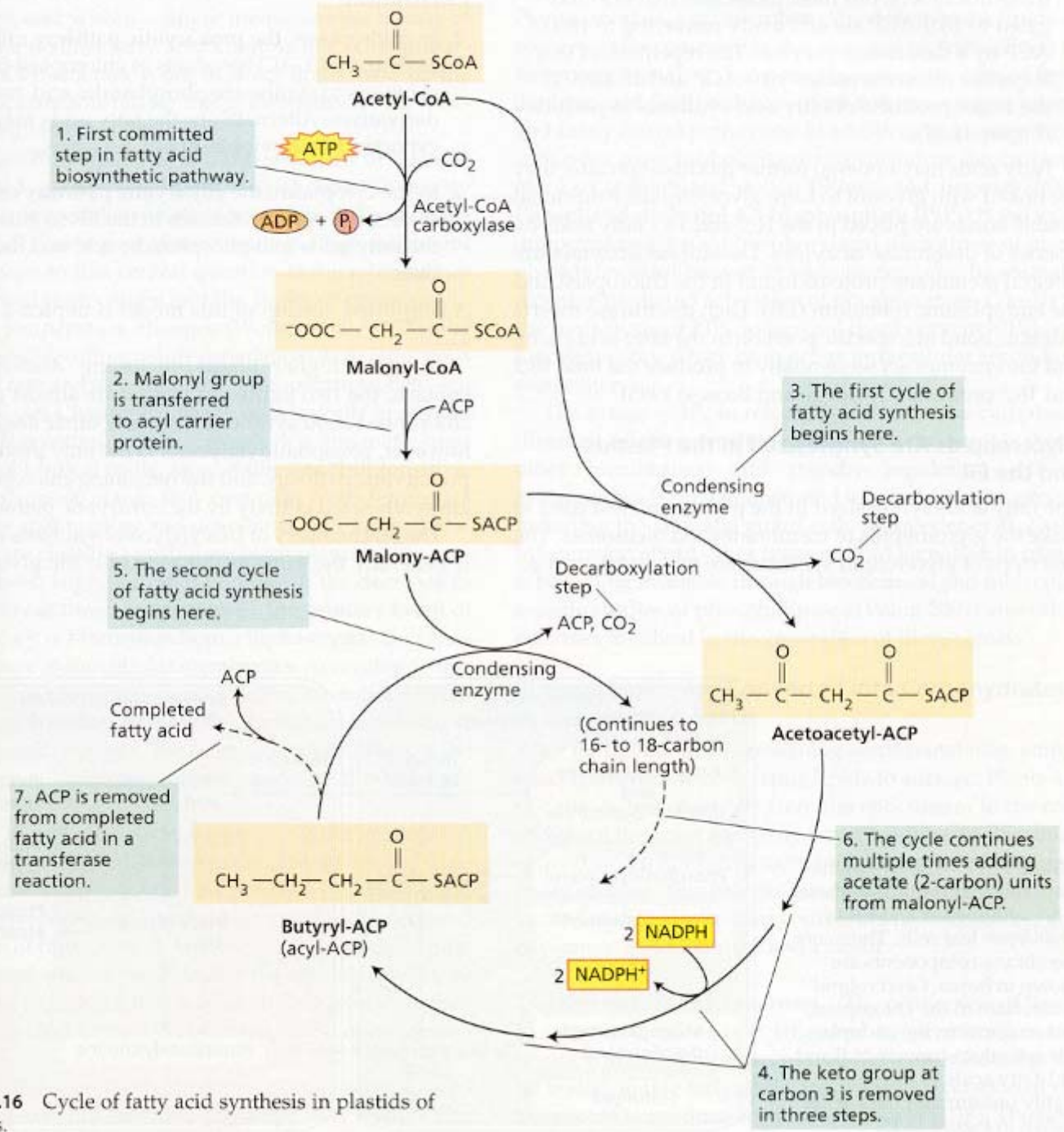

FIGURE 11.16 Cycle of fatty acid synthesis in plastids of plant cells.

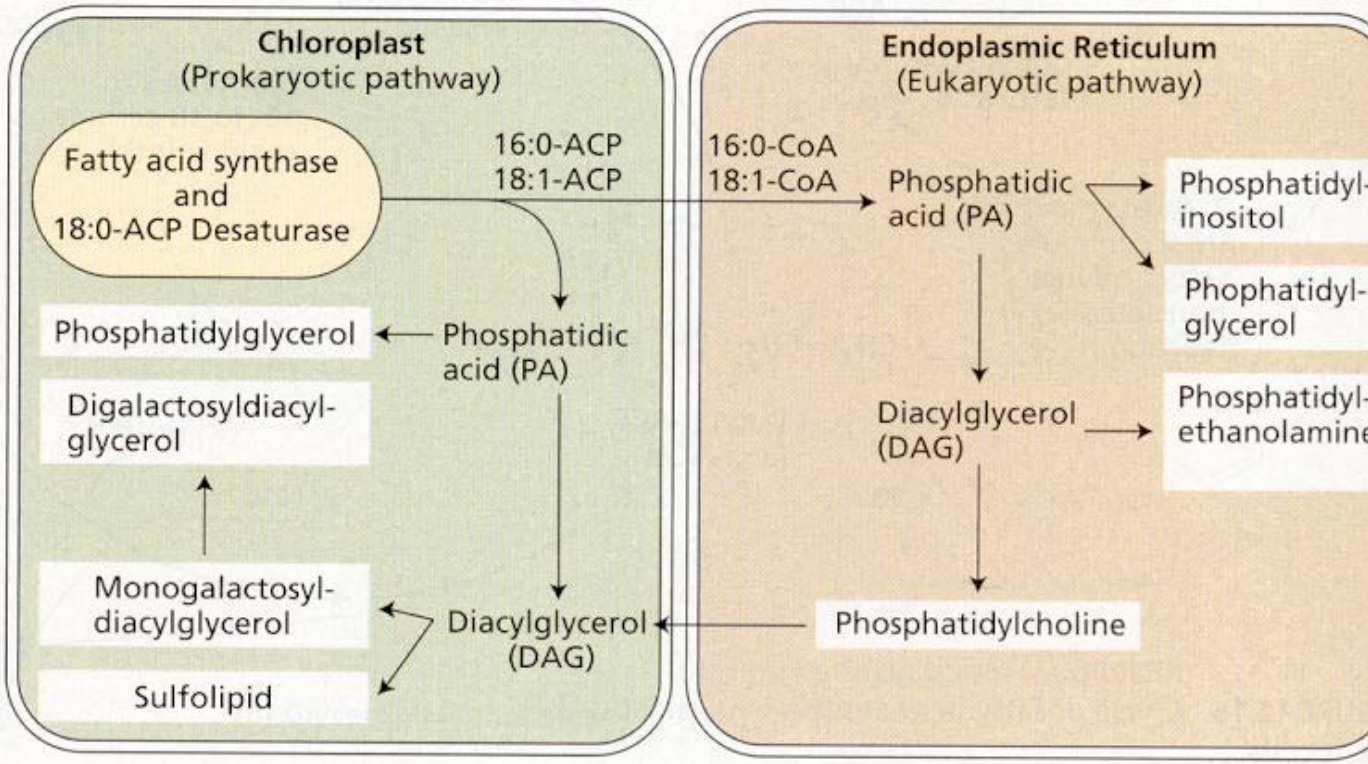

FIGURE 11.17 The two pathways for glycerolipid synthesis in the chloroplast and ER of *Arabidopsis* leaf cells. The major membrane components are shown in boxes. Glycerolipid desaturates in the chloroplast, and enzymes in the endoplasmic reticulum convert 16:0 and 18:1 fatty acids to the more highly unsaturated fatty acids shown in Figure 11.15.

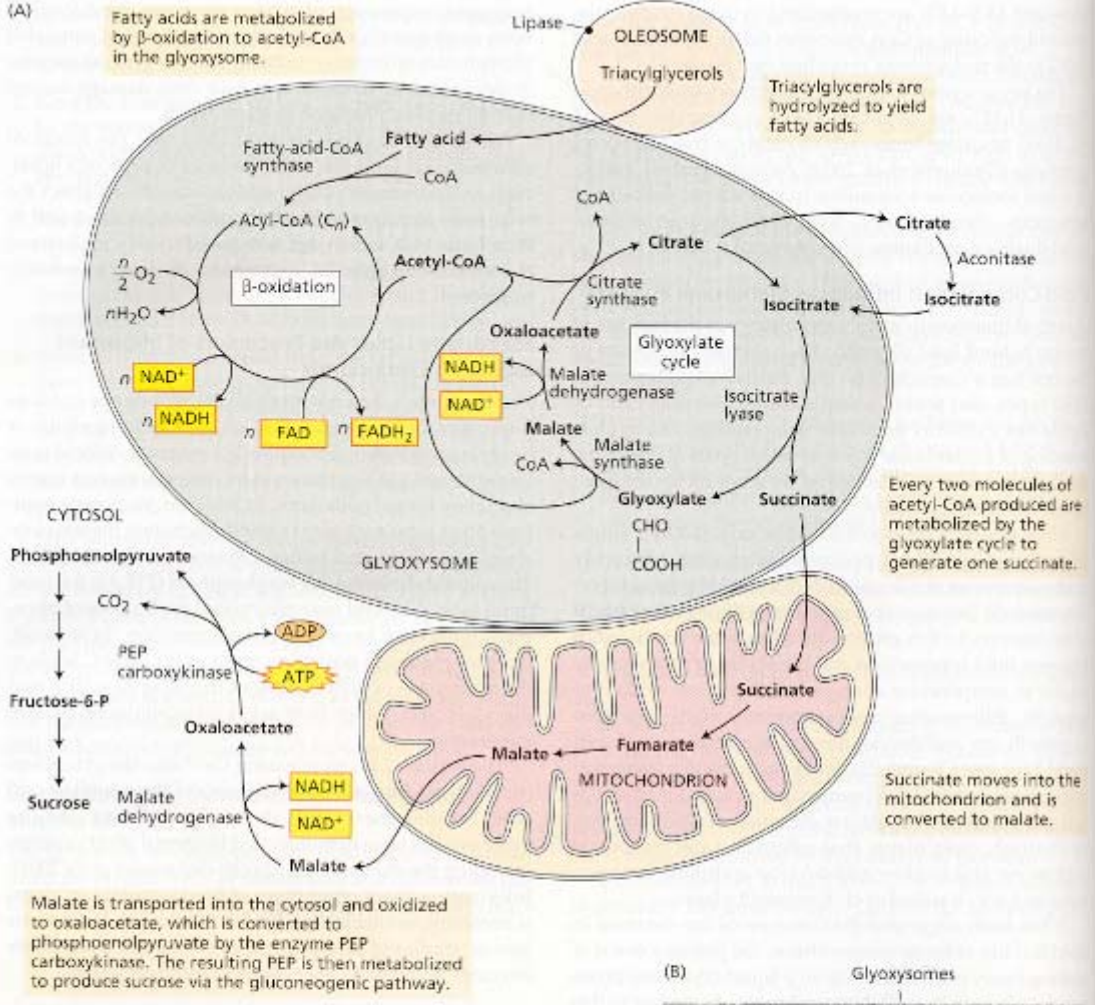

FIGURE 11.18 The conversion of fats to sugars during germination in oil-storing seeds. (A) Carbon flow during fatty acid breakdown and gluconeogenesis (refer to Figures 11.2, 11.3, and 11.6 for structures). (B) Electron micrograph of a cell from the oil-storing cotyledon of a cucumber seedling, showing glyoxysomes, mitochondria, and oleosomes. (Photo courtesy of R. N. Trelease.)